Hindawi Publishing Corporation
Journal of Sensors
Volume 2016, Article ID 3053019, 8 pages
http://dx.doi.org/10.1155/2016/3053019

Research Article

Development and Characterization of an Electroless Plated Silver/Cysteine Sensor Platform for the Electrochemical Determination of Aflatoxin B_1

Alex Paul Wacoo,[1,2] Mathew Ocheng,[3] Deborah Wendiro,[1] Peter California Vuzi,[2] and Joseph F. Hawumba[2]

[1]*Microbiology and Biotechnology Centre, Department of Product Development, Uganda Industrial Research Institute, P.O. Box 7086, Kampala, Uganda*
[2]*Department of Biochemistry and Sports Science, School of Biological Sciences, College of Natural Sciences, Makerere University, P.O. Box 7082, Kampala, Uganda*
[3]*Instrumentation Unit, Technology Development Centre, Uganda Industrial Research Institute, P.O. Box 7086, Kampala, Uganda*

Correspondence should be addressed to Joseph F. Hawumba; jhawumba@cns.mak.ac.ug

Received 25 March 2015; Revised 25 September 2015; Accepted 27 September 2015

Academic Editor: Banshi D. Gupta

An electroless plated silver/cysteine sensor platform [Glass|silver|cysteine|aflatoxin B_1|horseradish peroxidase] for the Electrochemical detection of aflatoxin B_1 was developed and characterized. This involved four major steps: (1) an electroless deposition of silver (plating) onto a glass slide, (2) immobilization of cysteine; (3) conjugation of aflatoxin B_1 to cysteine groups; and (4) blocking of free cysteine groups with horseradish peroxidase (HRP). The binding of cysteine to the silver was demonstrated by the disappearance of thiol (S-H) groups at 2500 cm^{-1} using Fourier transmittance infrared spectra (FT-IR), while the subsequent steps in the assembly of sensor platform were monitored using both FT-IR and cyclic voltammetry, respectively. The sensor platform exhibited a broadened nonsymmetrical redox couple as indicated by cyclic voltammetry. The platform was further characterized for sensitivity and limit of detection. The indirect competitive immunoassay format, whereby free and immobilized aflatoxin B_1 on the sensor competed for the binding site of free anti-aflatoxin B_1 antibody, was used at various concentrations of aflatoxin B_1. The sensor generated differential staircase voltammogram that was inversely proportional to the concentration of aflatoxin B_1 and aflatoxin B_1 in the range of 0.06–1.1 ng/mL with a detection limit of 0.08 ng/mL could be detected.

1. Introduction

Several methods have been described for the detection of aflatoxins in foodstuff and feeds [1]; including, among others, such methods as thin-layer chromatography (TLC), high-performance liquid chromatography (HPLC), and immunoassay based methods. Immunoassay methods, which became widely popular during late 1970s, rely on the specificity of binding between antibodies/receptors and antigens/ligands. The high affinity and specificity of antibodies/receptors for antigens/ligands have been used in the development of the various immunochemical methods [2]. The formation of either the antibody-antigen or the receptor-ligand complexes can be quantified by following the change in the absorbance of photons of light energy spectrophotometrically. In other instances, the binding events, as well as the resultant complexes, may require amplification for better signal recognition. This has been achieved by using various labels comprising enzymes (as for the enzyme-linked immunosorbent assay (ELISA)), fluorophores, and radioisotopes (as for the radioimmunoassay (RIA)), among others. The application of immunochemical methods for determining aflatoxin B_1 in peanuts was reported by Langone and Van Vunakis, [3] using solid phase radioimmunoassay (RIA). Several other investigators have also reported the use of monoclonal antibody in immunoaffinity column assay (ICA) and ELISA for

determining aflatoxins in peanuts [4]. The advantages of immunoassays included high level of specificity and sensitivity even in the presence of contaminating materials and ease of sample preparation, as well as usage and low cost. However, the requirement for molecular labels, expensive equipment, and cumbersome multiple washing steps necessitated the development of more user-friendly devices.

Thus, immunosensors, which are biosensors that also rely on either antigen-antibody or receptor/ligand interaction to generate detectable signals, were developed. As a matter of fact, Immunosensors have proved to be self-sufficient integrated devices that use biological recognition element retained in direct spatial contact with a transduction element, to provide precise quantitative or semiquantitative results [5]. Moreover, immunosensors exhibit high sensitivities, with detection limits below 0.1 ng/mL [6]. Several electrochemical immunosensors have been developed through immobilization of antibodies onto the surface of an electrode and have been reported for detection of aflatoxins [7–9]. Nevertheless, some of them require labels for electrochemical transduction. To overcome the requirement of a label, label-free biosensor platforms such as optical waveguide [10], surface plasmon resonance platforms [11, 12], and electrochemical immunosensor have been developed. Although the two label-free platforms are highly sensitive and with detectable ranges between 0.5 and 10 ng/mL for aflatoxins, the devices operating these platforms are still expensive and not deployable in the field [1]. The aim of the study was to develop and characterize an electroless plated silver/cysteine sensor platform operating on a label-free format, for the detection of aflatoxin B_1 in foodstuff and feeds, as well as the construction of a field-deployable devise operating on this platform appropriate for field analysis of aflatoxin B_1. The development and characterization of an electroless plated silver/cysteine sensor platform [glass|silver|cysteine|aflatoxin B_1|horseradish peroxidase-blocked] is herewith reported.

2. Materials and Methods

2.1. Reagents, Materials, and Apparatus. All chemicals and reagents used were purchased from Sigma and all were, unless stated, of analytical grade. Acetate buffer (0.1 M, pH 6.5) was prepared from stock solutions of CH_3COONa, CH_3COOH, and KCl. Silver ammonia ($Ag(NH_3)^+$) solution (5%, w/v) was prepared by dissolving 0.5 g of Silver nitrate in 10 mL of absolute ammonia solution. Sodium hydroxide (10%, w/v) was prepared by dissolving 5 g of NaOH in 50 mL of deionized water. Piranha solution contained 3 parts of concentrated sulphuric acid and 1 part of hydrogen peroxide in the ratio. D-glucose (5%, w/v) solution was prepared by dissolving 2.5 g of D-glucose in 50 mL of distilled water. L-cysteine (analytical purity) was obtained from Nutritional Biochemical Corporation (USA). A solution of 10 μM hydrogen peroxide was prepared from a stock solution of 30% (v/v) hydrogen peroxide solution. Aflatoxin B_1 standard solution (0.1–1.0 ng/mL) was prepared by serial dilution of aflatoxin B_1 stock solution (1 mg/mL) in phosphate buffer saline (PBS) containing 10% (v/v) methanol. The aflatoxin B_1 monoclonal antibody reagent contained 6.8 mg/mL of total protein in 0.15 M sodium azide (NaN_3) as preservative. The horseradish peroxidase (HRP) contained 169 units/mL of the lyophilized powder. Fourier Transform Infrared (FTIR) spectrophotometer (Perkin Elma, Massachusetts, USA) was used to generate FT-IR spectra. A three-electrode electrochemistry workstation developed locally at Instrumentation Unit, Technology Development Centre, Uganda Industrial Research Institute, was used to measure both cyclic voltammogram (CV) and differential staircase voltammogram (DSCV). The work station was connected to Arbitrary/Function Generator with counter (BK Precision, 4048, UK) and used to generate staircase and cyclic waves. Digital storage oscilloscope (BK Precision, 2540, UK) was used for data acquisition. Silver (Ag)/silver chloride (AgCl) (3 M) was used as a reference. The pH measurements were performed with 827 Metrohm pH meter (Mettler Toledo, Switzerland). Acidified Tin IV chloride solution contained 12 mg $SnCl_2$, 0.05 mL hydrochloric acid, and 49.95 mL deionized (DI) water. Acidified silver nitrate solution contained 4 mg $AgNO_3$, 0.05 mL HCl, and 49.95 mL DI water. Modified Tollen's plating reagent contained 20% (w/v) silver ammonia ($Ag(NH_3)^{2+}$) solution, 2.5 mL 10% (w/v) sodium hydroxide (NaOH), and 2.5 mL of 5% (w/v) D-glucose. Aflatoxin B_1 immobilisation reagent prepared by 20 mg of aflatoxin B_1 dissolved in mixture of pyridine, methanol, and water in a ratio of 1 : 4 : 1.

2.2. Development of a Biosensor Platform

2.2.1. Deposition of Silver on the Glass Slide. The first step in the development of the biosensor platform involved an electroless deposition of silver (plating) onto a glass slide (Figure 1, step 1). This is typically a wet chemical process that involved selective reduction of silver ions on a glass slide surface. Glass slides (0.4 × 1.5 cm) were immersed sequentially, for 5 min each, in deionized water and 95% (v/v) ethanol followed by removal of organic impurities in a freshly prepared Piranha solution at 90°C for 30 min. Thereafter, the slides were activated by Sn-Ag in a two-step process [13]. The slides were first activated in acidified solution of Tin IV chloride, rinsed with deionized water and subsequently sensitized in another acidified solution of Silver nitrate ($AgNO_3$) for 25 s. and finally rinsed, sequentially, in nitric acid containing deionized water, and with deionized water alone, to remove unbound Sn^{2+} compounds. The activated glass slides were immersed in 2 mL of modified Tollen's reagent plating solution and rinsed with DI water after 5 min. This step was repeated six times [14]. Thereafter, the coated slides were air dried and annealed at 300°C for 6 min in a furnace under the atmosphere nitrogen. The immobilized/coated silver served as the transducer of the sensor platform. The surface of the annealed coated silver was monitored by using FT-IR between 400 cm^{-1} and 4,000 cm^{-1} at a scanning speed of 500 nm/min.

2.2.2. Assembly of the Immunosensor. The second phase in the development of the immunosensor platform involved three major steps: (1) immobilization of cysteine; (2) conjugation

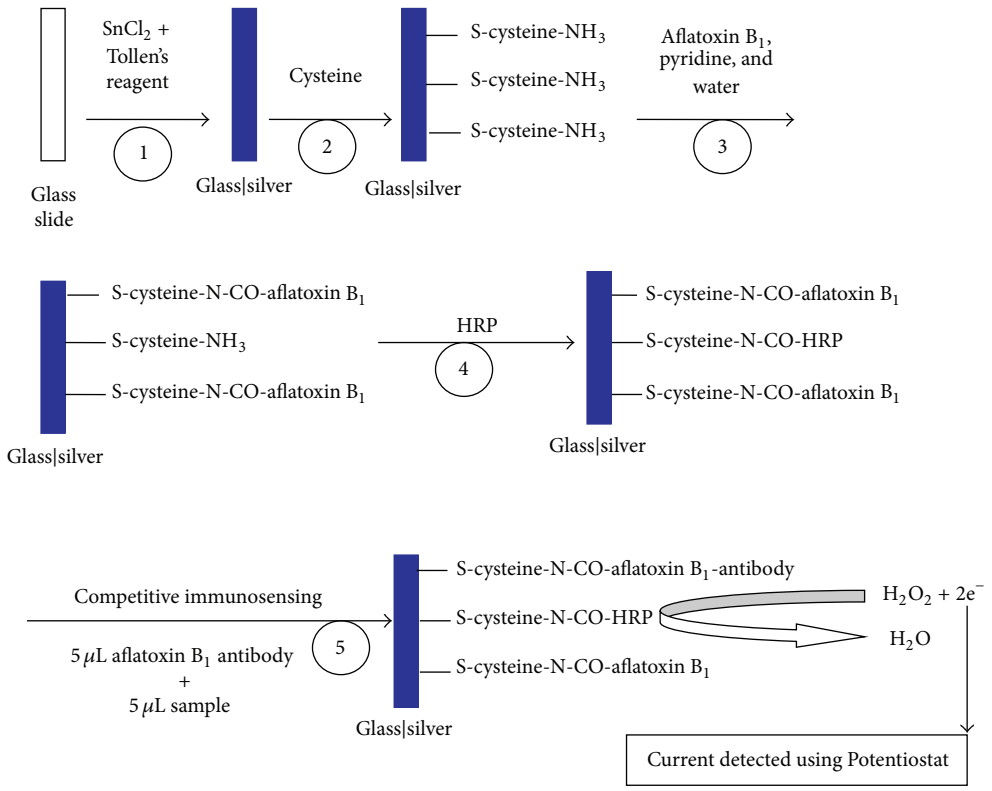

FIGURE 1: Representation of major steps in the assembly of the immunosensor platform. Step 1: electroless silver plating. Step 2: immobilization of cysteine. Step 3: conjugation of aflatoxin B_1 to cysteine groups. Step 4: blocking of aflatoxin B_1 layer with HRP. Step 5: competitive immunosensing of aflatoxin B_1.

of aflatoxin B_1 to cysteine groups; and (3) blocking of free cysteine groups (unconjugated to AFB1) with HRP. (Figure 1: steps 2 to 4). In order to functionalize the sensor platform, the annealed glass|silver was immersed in the saturated solution of L-cysteine for 12 h, rinsed with distilled water, and finally dried in a stream of nitrogen gas and stored at 4°C as it awaits conjugation step. The conjugation of aflatoxin B_1 to cysteine groups immobilized onto the silver (transducer) involved an overnight incubation of the cysteine-functionalized glass/silver platform in an aflatoxin B_1 immobilization reagent and thereafter the platform was washed several times in 0.1 M phosphate buffer of pH 7.4 to remove any residual monomer and weakly bound aflatoxin B_1 molecules. The unconjugated sites of cysteine on the resultant immunosensor platform were blocked by incubating it in 0.1 M acetate buffer (pH 6.5) containing 1 mg/mL HRP at 4°C for 15 hours. The sensor platform was subsequently washed in 0.1 M phosphate buffer (pH 7.4), dried in a stream of nitrogen, and stored at 4°C until used. To make certain that the blocking step was successful, the prensence of HRP enzymes at the blocked sites was assayed using hydrogen peroxide as a substrate. The sensor was treated with 10 μM hydrogen peroxide (H_2O_2) in citrate buffer, pH 6.5, and the activity of horseradish peroxidase, defined by its breakdown of H_2O_2 to water, oxygen, and two electrones, monitored by cyclic voltammetric scan. The scan was performed at a voltage ranging from 0 to −1000 mV at rate of 100 mV/s. The FT-IR spectra were measured between 400 cm^{-1} and 4,000 cm^{-1} at a scanning speed of 500 nm/min at every stage of sensor platform development. In order to ascertain that the change in the chromatogram when the electroless plated silver is conjugated to cysteine, FT-IR spectrum of cysteine alone was also measured between 400 cm^{-1} and 4,000 cm^{-1} at a scanning speed of 500 nm/min and plotted in the same graph for comparative purpose. For the electrochemical detection of aflatoxin B_1 using a competitive immunosensing format, the sensor platform (i.e., Glass|silver|cysteine|aflatoxin B_1|HRP-blocked) served as a working electrode. From henceforth, sensor electrode is synonymous to sensor platform.

2.3. Electrochemical Immune Detection of Aflatoxin B_1. In order to test the performance of the developed sensor platform for the detection of aflatoxin B_1, the sensor platform served as a working electrode and a competitive immunosensing format (Figure 1; step 5) was performed both in the absence and presence of free aflatoxin B_1 [6]. In the absence of free aflatoxin B_1, 5 μL aliquot of aflatoxin B_1 antibody was bound onto the sensor electrode for 5 min and then the sensor was transferred to another 5 mL cell solution of 10 μM H_2O_2 in 0.1 M acetate buffer pH 6.5. Differential staircase voltammetric measurement of the working electrode was performed by scanning from 0 to 600 mV at 60 mV pulse amplitude and 20 mV/s potential scan rate. For investigation in the presence of aflatoxin B_1, aliquots of 5 μL of anti-aflatoxin B_1 antibody solution were mixed with 5 μL

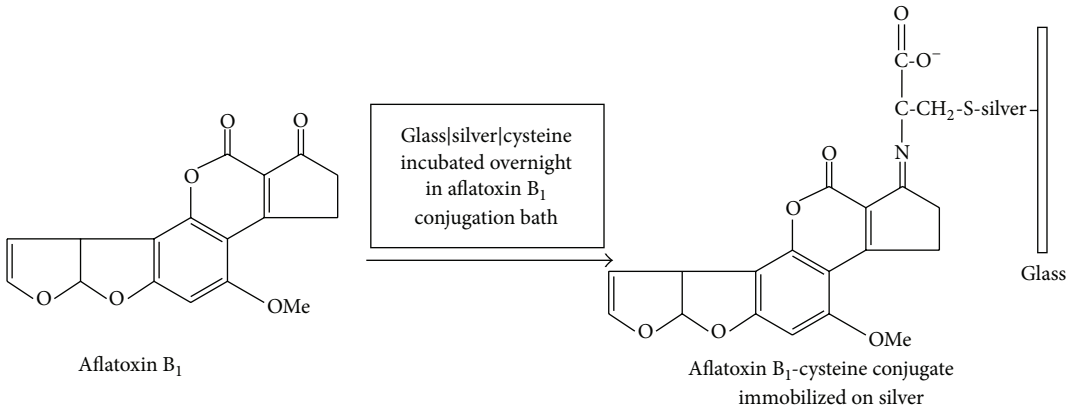

Figure 2: Preparation of aflatoxin B_1-cysteine-silver conjugate.

each of 0.2, 0.5, 0.8, and 1.0 ng/mL standard aflatoxin B_1 in 70% (v/v) methanol and 5 μL each of the mixtures placed on sensor platform and allowed to react for 5 min. This was followed by differential staircase voltammetric measurement as described above. In order to calibrate the sensor platform, the same experiment was repeated in triplicate and the peak heights at each concentration were plotted to obtain three calibration curves. The correlation coefficient (R^2) and slope of the regression line of each curve were determined, and the limit of detection (LOD) was calculated from LOD = (3.3 $*$ SD)/slope, where SD equals the standard deviation of correlation coefficient of 3 calibration curves and slope equals the mean of the slopes of the 3 calibration curves.

2.4. Determination of the Stability and Specificity of the Sensor Platform. The stability of the sensor platform was monitored every week for a period of 5 weeks by determining 0.2 ng/mL of aflatoxin B_1 as described above (Section 2.3). In order to determine the specificity of the immunosensor platform, aliquots of 0.5 μL each of the interfering aflatoxin molecules such as aflatoxin B_2, aflatoxin G_1, and aflatoxin G_2 at a concentration of 1 ng/mL were mixed with 0.5 μL of aflatoxin B_1 and a concentration of 0.2 ng/mL and the concentration of aflatoxin B_1 estimated as described before (Section 2.3). This was repeated three times.

3. Results and Discussion

3.1. Development and Characterizations of the Immunosensor Platform. The sensor platform was developed as described in materials and methods (Sections 2.1 and 2.2). The first step involved an electroless plating of silver metal, which would later function as an electron transducer onto glass plates. In order to functionalize the plated silver, cysteine was linked to the silver surface via the thiol group, which, in turn, resulted in the formation of amine-terminated self-assembled monolayer of cysteine residues. The amino groups of self-assembled monolayer of the cysteine residues are thus available for conjugation to aflatoxin B_1 as illustrated in Figure 2.

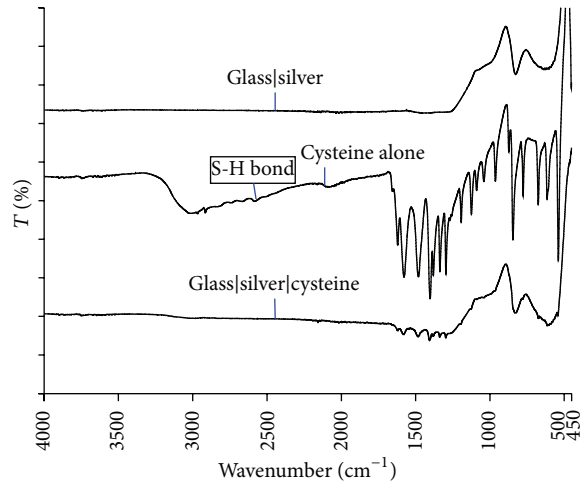

Figure 3: FT-IR spectra of electroless silver, cysteine, and glass|silver|cysteine demonstrating glass plated with silver, standard cysteine, and cysteine immobilized on the silver by using thiol group.

The sensor platform was characterized at every step during its development, as described in Materials and Methods (Sections 2.1 and 2.2). Fourier transmittance infrared spectra (FT-IR) was performed after every step, that is, electroless silver plating, formation of self-assembled monolayer of cysteine on silver (conjugation), conjugation of aflatoxin B_1 to cysteine group, and after blocking of the unconjugated cysteine residue sites with HRP (Figure 3). The formation of a sulfur-silver bond was demonstrated by the vanishing of a 2500 cm^{-1} peak of the combined spectrum of the conjugated silver/cysteine. This peak is only present in free cysteine as seen in Figure 1 (cysteine) due to the presence of thiol (S-H) bond. However, this peak was not recorded in the FT-IR spectrum of glass-silver-cysteine, due the formation of an S-Ag bond between plated silver and cysteine instead of the S-H bond in free cysteine [15, 16]. Further confirmation of the presence of cysteine binding to the silver was demonstrated by carboxylate (-COOH) stretch vibration of cysteine recorded around 1440–1640 cm^{-1} as shown in Figure 3.

In order to investigate the signal transduction of assembled immunosensor, the electrical signal generation was monitored by cyclic voltammetry at each of the steps of development of the bisensor in 0.1 M acetate buffer pH 6.5 containing 0.1 M potassium chloride and 10 μM H_2O_2 (Figure 2). The unplated glass slide did not generate any redox potential over the entire scan from −1000 to 0 mV (Figure 4(a)). The electroless-silver-plated glass [glass|silver] generated a reversible electrochemical potentialwith the anodic peak output potential magnitude of 240 mV and cathodic peak potential of 1920 mV and peak separation of ~200 mV at 100 mV/s (Figure 4(b)). This was because silver is a good conductor of electricity and the oxidation of silver to silver oxide and resultant reduction of silver oxide to silver led to the increase in the magnitude of redox couple [17]. However, the magnitude of the response potential decreased slightly to 160 mV (Figure 4(c)) after conjugation of L-cysteine onto the silver. The slight decrease in response suggests that the binding of cysteine does not affect the overall electron transfer on the sensor electrode [18]. However, a large reduction was observed from 160 mV to −250 mV after the binding of aflatoxin B_1 onto the sensor electrode (Figure 4(d)), indicating that the binding of aflatoxin B_1 on the surface of the glass|silver|cysteine sensor electrode blocked both electron and mass transfer. Nevertheless, the peak potential was restored to 160 mV after blocking with horseradish peroxidase (step 4; Figure 1). This could be attributed to the catalytic action of immobilised HRP that oxidize H_2O_2 to oxygen and water in a reaction accompanied by the release of 2 moles of electrons. The electrons thus generated should account for restoration of the electrical potential to 160 mV.

3.2. Performance of the Electrochemical Immunosensor. During the development of the sensor platform, the active sites of cysteine provided by amino groups of silver|cysteine|aflatoxin B_1 were blocked using HRP to prevent nonspecific binding of aflatoxin B_1. Hydrogen peroxide (H_2O_2), a substrate of HRP, was used to establish whether the enzyme was bound on the free cysteine residues and thus immobilised onto the sensor electrode. Cyclic voltammogram of aflatoxin B_1 immunosensor in acetate buffer (PH 6.5) in the absence (A) and presence (B) of H_2O_2 is shown in Figure 5. Although both the cathodic (reduction of silver takes place) and the anodic (oxidation of silver takes place) peaks (Figure 5(A)) observed in the absence of H_2O_2 were long-drawn-out, the same peaks (Figure 5(B)) were broadened and nonsymmetrical in the presence of H_2O_2. The long-drawn-out peaks suggested that redox reactions involving formation of silver oxide occurred on the surface of the sensor electrode [17]. Such reactions were markedly reduced, which resulted in the decrease in the cathodic and anodic peaks in the presence of 10 μM H_2O_2 (Figure 5(B)) indicative of successful binding of HRP onto the surface of the sensor electrode.

In order to test the performance of the developed sensor platform for the detection of aflatoxin B_1, the sensor platform served as a working electrode and a competitive immunosensing format (Figure 1; step 5) was performed both in the absence and presence of free aflatoxin B_1 (Section 2.3). The performance of the sensor electrode in the detection of varying concentrations of aflatoxins was tested using different concentrations of aflatoxin B_1 (0-1 ng/L) and differential staircase voltammogram (DSCV) [19] was used for the determination of aflatoxin B_1 (Figure 6). Figure 6 shows that the DSCV currents increase with a decrease in aflatoxin B_1 concentrations, suggesting that the peak potential is inversely proportional to aflatoxin B_1 concentration. This observation suggested that the increased formation of the antigen (aflatoxin B_1) antibody complexes with the increase in aflatoxin B_1 concentration may have shielded the active sites of HRP making it inaccessible to H_2O_2. This inhibition of the breakdown of H_2O_2 should have caused a parallel decrease in electron transfer on the sensor platform [11], hence the observed inverse relation between the potentials generated as the concentration aflatoxin B_1 increase (Figure 6).

The calibration of the immunosensor platform showed that it operates within a linear dynamic range (DLR) from 0.06 to 1.1 ng/mL aflatoxin B_1 concentration, with a limit of detection (LOD) of 0.08 ng/mL. A comparison of the sensor platform with other electrochemical immunosensors for aflatoxin B_1 detection is presented in Table 1. As noted, the DLR and LOD values of the sensor platform, [glass|silver|cysteine|aflatoxin B_1|HRP-blocked], compare very well and in good agreement with other immunosensors reported [6, 7, 20, 21].

3.3. Stability and Selectivity of the Immunosensor. The stability of this sensor was monitored every week for a period of five weeks. The differential staircase voltammogram (DSCV) response of the sensor changed from 1066.7 ± 46.2 mV to 1040 ± 144.2 mV which is approximately 2.5% after three weeks, and thereafter it decreased, 1000 ± 40 mV (which is 6.3%) and 960 ± 80 mV (which is 10%), respectively, at the fourth and fifth week (Figure 7). This suggested that the sensor platform can effectively be used for aflatoxin B_1 and determination within two weeks without loss of accuracy. Perhaps this period may be extended if the frequency of use is low.

The determination of the response of the sensor platform to interference or crossing recognition levels and to the coexisting molecules in sample was monitored as described above (Section 2.4). There was a slight interference in the detection of aflatoxin B_1 in the presence of aflatoxin G_2 (i.e., 1.44%, which is 60 mV of the 4160 mV determined for pure aflatoxin B_1), followed by aflatoxin B_2 (i.e., 8.65%, which is 360 mV of the 4160 mV determined for pure aflatoxin B_1) (Figure 8). Aflatoxin G_1 interfered more with the determinations of aflatoxin B_1 (i.e., 18.2%, which is 760 mV of the 4160 mV determined for pure aflatoxin B_1) (Figure 8), suggesting that the two could have structural similarities especially in areas that recognize the antibodies. However, since five times the concentration of aflatoxin B_1 was used for each interfering molecule, it suggests that, in the excess of aflatoxin B_1, none of those contaminants would be detected, which, in turn,

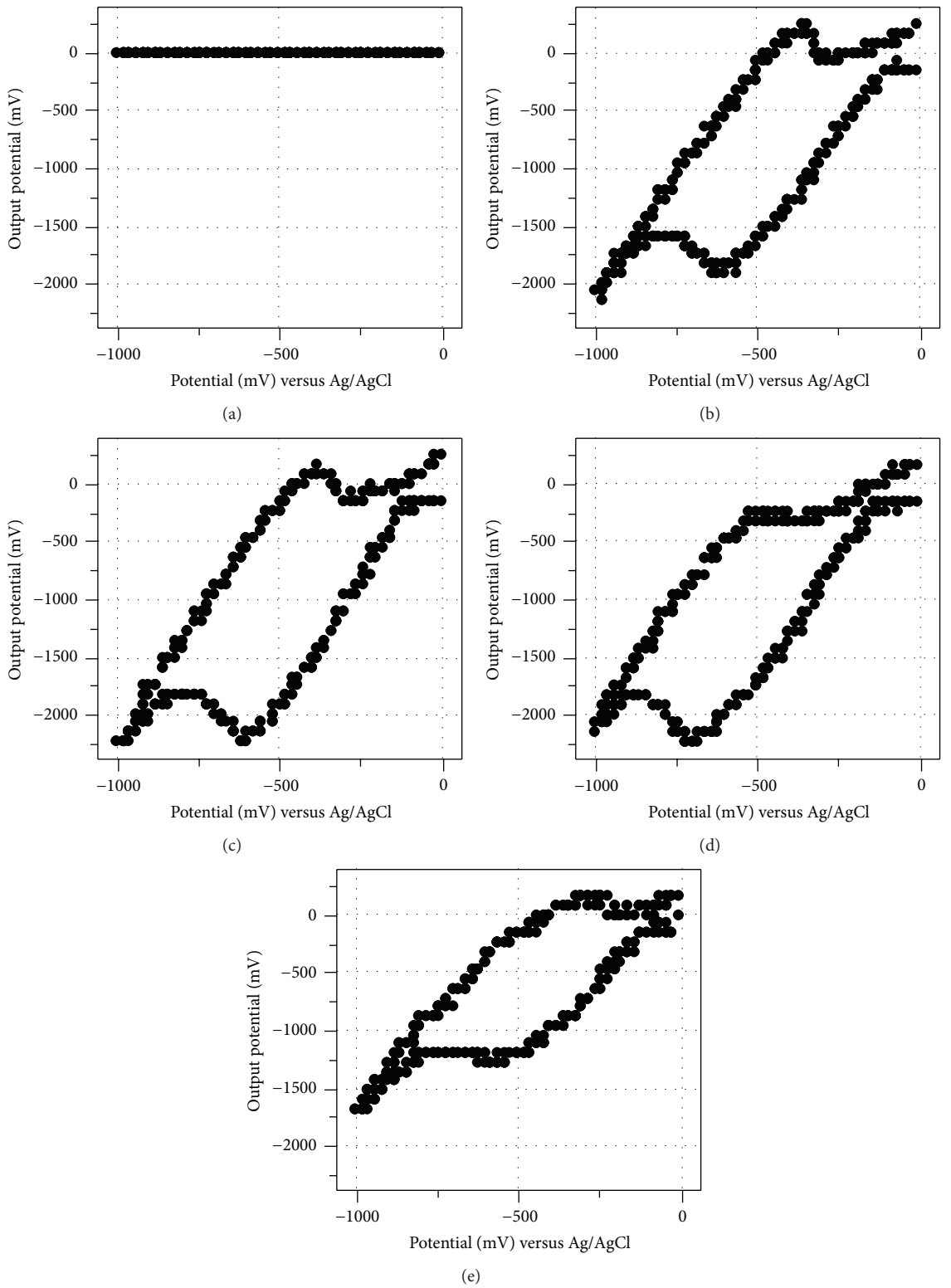

Figure 4: Cyclic Voltammogram of (a) bare glass; (b) glass|silver; (c) glass|silver|cysteine|; (d) glass|silver|cysteine|aflatoxin B_1; (e) glass|silver|cysteine|aflatoxin B_1|HRP-blocked (Scan rate: 100 mV/s).

Table 1: Comparison of DLR and LOD of different aflatoxin B_1 immunosensors.

Electrochemical immunosensors	DLR (ng/mL)	Limit of detection (ng/mL)	Reference
GCE/AuNP/PTH/aflatoxin B_1-BSA-conjugate/HRP-blocked	0.6–2.4	0.07	[6]
BSA/aAFB_1-C-AuNP/MBA/Au	0.01–0.1	0.0179	[20]
Pt/PSSA/PANI/anti-aflatoxin B_1	0.1–0.6	0.1	[21]
GCE/chitosan/AuNP/anti-aflatoxin B_1	0.6–110	0.2	[7]
Glass|silver|cysteine|aflatoxin B_1|HRP-blocked	0.06–1.1	0.08	This work

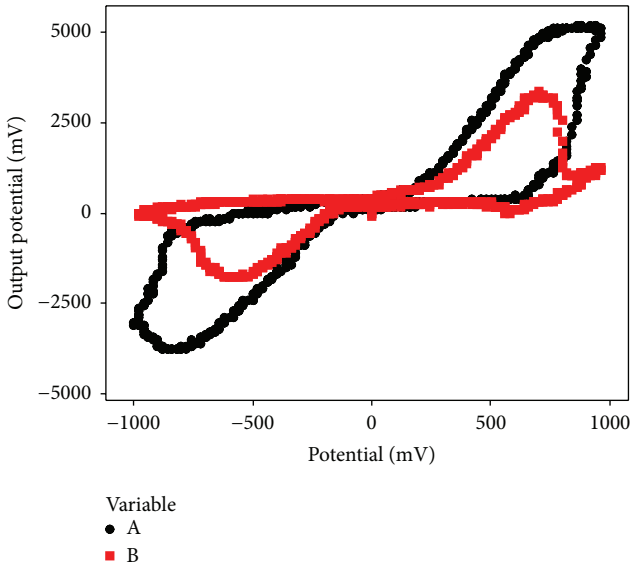

Figure 5: Cyclic voltammogram of Aflatoxin B_1 immunosensor in acetate buffer (PH 6.5) in the absence (A) and presence (B) of H_2O_2 (scan rate: 100 mV/s).

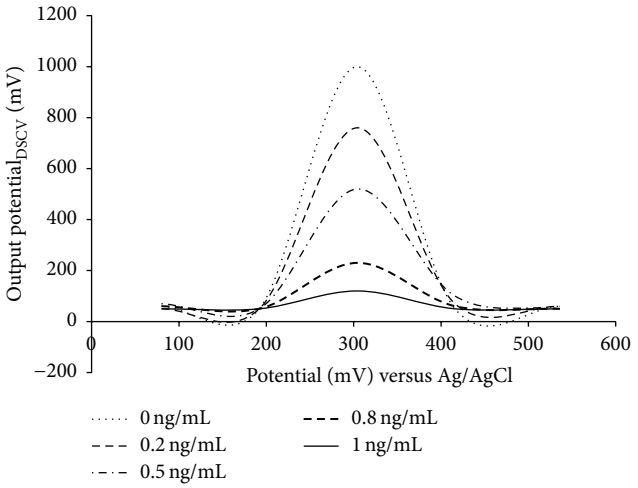

Figure 6: DSCV response recorded for silver|cysteine|aflatoxin B_1|HRP-blocked immunoelectrode for 0-1 ng/mL of aflatoxin B_1 concentrations in a pH 6.5 acetate buffer solution (scan rate of 20 mV/s).

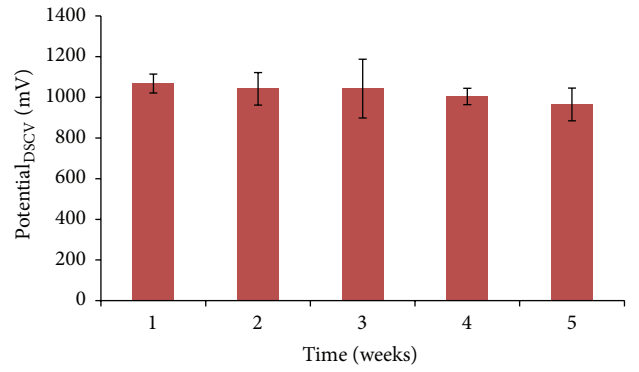

Figure 7: The stability of the electrochemical immunosensor observed in a period of five weeks. The differential staircase voltammogram (DSCV) response of the sensor was monitored every week for five weeks and the DSCV value was fairly stable.

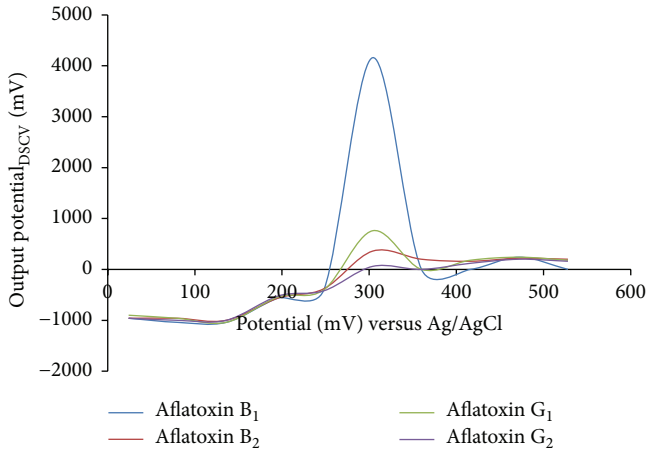

Figure 8: The specificity of the immunosensor platform toward aflatoxin B_1, aflatoxin B_2, aflatoxin G_1, and aflatoxin G_2.

suggests that the newly developed sensor platform is highly specific for aflatoxin B_1.

4. Conclusion

An electroless plated silver/cysteine sensor platform [glass|silver|cysteine|aflatoxin B_1|horseradish peroxidase] for the electrochemical detection of aflatoxin B_1 has successfully been developed and characterized, and its performance is

demonstrated. The limit of detection and linear dynamic range of this sensor platform are comparable to those of other immunosensors used for aflatoxin B_1 analysis. To the best of our knowledge, this is the first work that utilises electroless plated silver technology in the construction of a sensor platform for aflatoxin analyses. While these preliminary findings indicated that this immunosensor platform can be used to build an inexpensive electrochemical biosensor device for field use, this must wait for validation of its performance using HPLC as the gold standard method. This work is currently in progress.

Conflict of Interests

The authors declare that there is no conflict of interests regarding the publication of this paper.

Acknowledgments

The authors acknowledge the financial support from the Canadian International Development Research Council (IDRC) and Uganda Industrial Research Institute (UIRI), and the technical support from the Department of Chemistry, UIRI, and the Department of Chemistry, Uganda Bureau of Standards (UNBS).

References

[1] A. P. Wacoo, D. Wendiro, P. C. Vuzi, and J. F. Hawumba, "Methods for detection of aflatoxins in agricultural food crops," *Journal of Applied Chemistry*, vol. 2014, Article ID 706291, 15 pages, 2014.

[2] A. Sargent and O. A. Sadik, "Monitoring antibody–antigen reactions at conducting polymer-based immunosensors using impedance spectroscopy," *Electrochimica Acta*, vol. 44, no. 26, pp. 4667–4675, 1999.

[3] J. J. Langone and H. Van Vunakis, "Aflatoxin B; specific antibodies and their use in radioimmunoassay," *Journal of the National Cancer Institute*, vol. 56, no. 3, pp. 591–595, 1976.

[4] D. Babu, *Rapid and Sensitive Detection of Aflatoxin in Animal Feeds and Food Grains Using Immunomagnetic Bead Based Recovery and Real-Time Immuno Quantitative Pcr (Rt-iqpcr) Assay*, Oklahoma State University, 2010.

[5] D. R. Thevenot, K. Toth, R. A. Durst, and G. S. Wilson, "Electrochemical biosensors: recommended definitions and classification," *Pure and Applied Chemistry*, vol. 71, pp. 2333–2348, 1999.

[6] J. H. O. Owino, O. A. Arotiba, N. Hendricks et al., "Electrochemical immunosensor based on polythionine/gold nanoparticles for the determination of aflatoxin B_1," *Sensors*, vol. 8, no. 12, pp. 8262–8274, 2008.

[7] L. Masoomi, O. Sadeghi, M. H. Banitaba, A. Shahrjerdi, and S. S. H. Davarani, "A non-enzymatic nanomagnetic electro-immunosensor for determination of aflatoxin B_1 as a model antigen," *Sensors and Actuators B: Chemical*, vol. 177, pp. 1122–1127, 2013.

[8] Z. Linting, L. Ruiyi, L. Zaijun, X. Qianfang, F. Yinjun, and L. Junkang, "An immunosensor for ultrasensitive detection of aflatoxin B_1 with an enhanced electrochemical performance based on graphene/conducting polymer/gold nanoparticles/the ionic liquid composite film on modified gold electrode with electrodeposition," *Sensors and Actuators, B: Chemical*, vol. 174, pp. 359–365, 2012.

[9] Y. Liu, Z. Qin, X. Wu, and H. Jiang, "Immune-biosensor for aflatoxin B_1 based bio-electrocatalytic reaction on micro-comb electrode," *Biochemical Engineering Journal*, vol. 32, no. 3, pp. 211–217, 2006.

[10] N. Adányi, I. A. Levkovets, S. Rodriguez-Gil, A. Ronald, M. Váradi, and I. Szendrő, "Development of immunosensor based on OWLS technique for determining Aflatoxin B1 and Ochratoxin A," *Biosensors and Bioelectronics*, vol. 22, no. 6, pp. 797–802, 2007.

[11] S. J. Daly, G. J. Keating, P. P. Dillon et al., "Development of surface plasmon resonance-based immunoassay for aflatoxin B_1," *Journal of Agricultural and Food Chemistry*, vol. 48, no. 11, pp. 5097–5104, 2000.

[12] L. Dunne, S. Daly, A. Baxter, S. Haughey, and R. O'Kennedy, "Surface plasmon resonance-based immunoassay for the detection of aflatoxin B_1 using single-chain antibody fragments," *Spectroscopy Letters*, vol. 38, no. 3, pp. 229–245, 2005.

[13] J. H. Byeon and J.-W. Kim, "Fabrication of a pure, uniform electroless silver film using ultrafine silver aerosol particles," *Langmuir*, vol. 26, no. 14, pp. 11928–11933, 2010.

[14] A. Antonello, B. Jia, Z. He et al., "Optimized electroless silver coating for optical and plasmonic applications," *Plasmonics*, vol. 7, no. 4, pp. 633–639, 2012.

[15] J. H. Priester, A. Singhal, B. Wu, G. D. Stucky, and P. A. Holden, "Integrated approach to evaluating the toxicity of novel cysteine-capped silver nanoparticles to *Escherichia coli* and *Pseudomonas aeruginosa*," *Analyst*, vol. 139, no. 5, pp. 954–963, 2014.

[16] A. C. Templeton, S. Chen, S. M. Gross, and R. W. Murray, "Water-soluble, isolable gold clusters protected by tiopronin and coenzyme a monolayers," *Langmuir*, vol. 15, no. 1, pp. 66–76, 1999.

[17] Y.-J. Choi and T.-J. M. Luo, "Electrochemical properties of silver nanoparticle doped aminosilica nanocomposite," *International Journal of Electrochemistry*, vol. 2011, Article ID 404937, 6 pages, 2011.

[18] Y. Liu and C. Feng, "A sensitive potentiometric immunosensor based on nano-gold/cysteine/nafion-modified platinum disk electrode," *International Journal of Digital Content Technology and its Applications*, vol. 7, no. 7, pp. 569–577, 2013.

[19] F. Scholz, L. Nitschke, and G. Henrion, "Differential staircase voltammetry—a new electroanalytical technique," *Fresenius' Zeitschrift für Analytische Chemie*, vol. 332, no. 7, pp. 805–808, 1988.

[20] A. Sharma, Z. Matharu, G. Sumana, P. R. Solanki, C. G. Kim, and B. D. Malhotra, "Antibody immobilized cysteamine functionalized-gold nanoparticles for aflatoxin detection," *Thin Solid Films*, vol. 519, no. 3, pp. 1213–1218, 2010.

[21] J. H. O. Owino, A. Ignaszak, A. Al-Ahmed et al., "Modelling of the impedimetric responses of an aflatoxin B1 immunosensor prepared on an electrosynthetic polyaniline platform," *Analytical and Bioanalytical Chemistry*, vol. 388, no. 5-6, pp. 1069–1074, 2007.